BIOCHEMISTRY
including biophysical chemistry & molecular biology

Article

pubs.acs.org/biochemistry

Analysis of the Interaction of Tarantula Toxin Jingzhaotoxin-III (β-TRTX-Cj1α) with the Voltage Sensor of Kv2.1 Uncovers the Molecular Basis for Cross-Activities on Kv2.1 and Nav1.5 Channels

Huai Tao,[†,‡] Jin J. Chen,[§] Yu C. Xiao,[†] Yuan Y. Wu,[†] Hai B Su,[†] Dan Li,[†] Heng Y. Wang,[†] Mei C. Deng,[∥] Mei C. Wang,[†] Zhong H. Liu,[†] and Song P. Liang*[,†]

[†]Key Laboratory of Protein Chemistry and Developmental Biology of Ministry of Education, College of Life Sciences, Hunan Normal University, Changsha, Hunan 410081, China

[‡]Department of Biochemistry and Molecular Biology, Hunan University of Chinese Medicine, Changsha, Hunan 410208, China

[§]College of Biology Science and Technology, Hunan Agricultural University, Changsha, Hunan 410128, China

[∥]Department of Biochemistry, School of Biological Science and Technology, Central South University, Changsha, Hunan 410013, China

Supporting Information

ABSTRACT: Animal venoms contain a fascinating array of divergent peptide toxins that have cross-activities on different types of voltage-gated ion channels. However, the underlying mechanism remains poorly understood. Jingzhaotoxin-III (JZTX-III), a 36-residue peptide from the tarantula *Chilobrachys jingzhao*, is specific for Nav1.5 and Kv2.1 channels over the majority of other ion channel subtypes. JZTX-III traps the Nav1.5 DII voltage sensor at closed state by binding to the DIIS3-S4 linker. In this study, electrophysiological experiments showed that JZTX-III had no effect on five voltage-gated potassium channel subtypes (Kv1.4, Kv3.1, and Kv4.1−4.3), whereas it significantly inhibited Kv2.1 with an IC_{50} of 0.71 ± 0.01 μM. Mutagenesis and modeling data suggested that JZTX-III docks at the Kv2.1 voltage-sensor paddle. Alanine replacement of Phe274, Lys280, Ser281, Leu283, Gln284, and Val288 could decrease JZTX-III affinity by 7-, 9-, 34-, 12-, 9-, and 7-fold, respectively. Among them, S281 is the most crucial determinant, and the substitution with Thr only slightly reduced toxin sensitivity. In contrast, a single conversion of Ser281 to Ala, Phe, Ile, Val, or Glu increased the IC_{50} value by >34-fold. Alanine-scanning mutagenesis experiments indicated that the functional surface of JZTX-III bound to the Kv2.1 channel is composed of four hydrophobic residues (Trp8, Trp28, Trp30, and Val33) and three charged residues (Arg13, Lys15, and Glu34). The bioactive surfaces of JZTX-III interacting with Kv2.1 and Nav1.5 are only partially overlapping. These results strongly supported the hypothesis that animal toxins might use partially overlapping bioactive surfaces to target the voltage-sensor paddles of two different types of ion channels. Increasing our understanding of the molecular mechanisms of toxins interacting with voltage-gated sodium and potassium channels may provide new molecular insights into the design of more potent ion channel inhibitors.

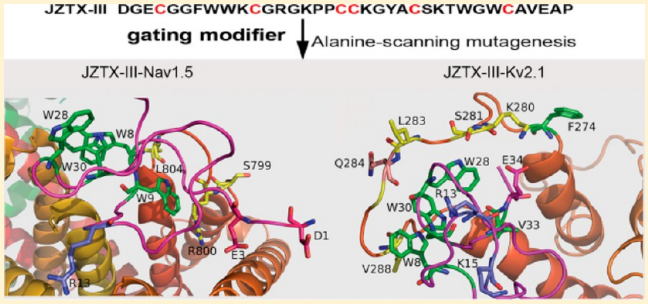

Voltage-gated potassium channels (VGPCs) are tetrameric membrane proteins that respond to changes in the transmembrane potential with conformational alterations that lead to the opening or closing of voltage-gated K^+ channels.[1,2] Each subunit contains six transmembrane segments (S1−S6). On the basis of distinct functional behaviors during channel activity, the six transmembrane segments are generally separated into the central pore domain and the voltage-sensing domains (VSDs) that are formed by the S1 through S4 segments.[3−7] VGPCs regulate many fundamental physiological processes, including action potential repolarization, hormone secretion, and neurotransmitter release, making them attractive pharmacological targets for binding distinct channel inhibitors.[8,9]

Studying the mechanisms of action of Kv inhibitors leads to a better understanding of the structure, function, and pharmacology of specific ion channels. By far, external pore block, internal cavity block, and voltage sensor trapping are three well-known mechanisms of blocking VGPCs.[10−12] In contrast to the scorpion toxin BmP01 that inhibits the hKv1.3 channel by docking onto the channel turret,[13] Hanatoxin1 (HaTx1) alters Kv2.1 channel gating by a voltage sensor trapping mechanism through binding to residues in the C-terminal portion of S3(S3b) of Kv2.1[14−16] and stabilizes the voltage sensor in the

Received: May 21, 2013
Revised: August 30, 2013
Published: September 17, 2013

dx.doi.org/10.1021/bi4006418 | *Biochemistry* 2013, 52, 7439−7448

resting state.[17] The voltage-sensor paddle is a region of Kv channels that is widely targeted by gating modifier toxins.[11] However, although another Kv2.1 gating modifier toxin, Guangxitoxin-1E (GxTX-1E), also targets the Kv2.1 S3b-S4 paddle through an interaction mechanism similar to that of HaTx1,[17,18] it fails to share the major determinant with HaTx1.[15,19] Moreover, the positions of determinants responsible for the binding of these gating modifier toxins do not completely overlap either.[14,15,17,19] Therefore, the structure determinants of the receptors and the molecular basis for gating modifier toxins interacting with Kv2.1 remain to be further defined.

Previous studies indicated that the S3−S4 linker of the voltage-gated ion channel is an important "hot spot" for the binding of gating modifier toxins.[20] The selectivity of many of the gating modifier toxins is promiscuous because of conserved three-dimensional structures existing within or across the ion channel families.[21−23] However, although the toxin-binding motifs are structurally conserved, the composition and arrangement of crucial receptor residues at corresponding positions in the voltage sensor are quite divergent. Thus, searching for the subtle differences in toxin-binding motifs that contribute to altered modes of action may be useful for a better understanding of the molecular details regarding toxin−channel interactions.

Jingzhaotoxin-III (JZTX-III), or β-theraphotoxin-Cj1α (β-TRTX-Cj1α), is isolated from the Chinese tarantula *Chilobrachys jingzhao*.[24] The toxin is a gating modifier of Kv2.1 and Nav1.5 channels without affecting the majority of other channel subtypes,[24−26] and electrophysiological studies showed that JZTX-III docked at the Nav1.5 DII S3−S4 linker.[27] JZTX-III is distinct from other voltage sensor toxins in its binding specificity and special molecular mechanism, making it a perspective molecular tool for better understanding the toxin−channel interaction. In this study, we investigated the molecular determinants and mode of action of JZTX-III targeting Kv2.1. Our data indicated that the binding of JZTX-III differs in that it shares only overlapping determinants on the voltage sensor with other Kv2.1 gating modifier toxins, with S281 being a major binding determinant. Interestingly, we also determined that JZTX-III interacts with Nav1.5 and Kv2.1 through distinct toxin−paddle interfaces, although the binding motifs and molecular mechanisms of the toxin targeting these two different types of ion channels are very similar. Our results provided new insights into conserved toxin-binding motifs that allow voltage sensor toxins to recognize ion channels with almost similar mechanisms of action but with partially overlapping bioactive surfaces.

EXPERIMENTAL PROCEDURES

Native JZTX-III Preparation. Spider venom was collected from the male and female spiders of *Chilobrachys jingzhao* by using an electro-pulse stimulator. Native JZTX-III was purified from the crude venom of the Chinese tarantula *Chilobrachys jingzhao* as described by Xiao et al.[24] Toxin was purified by a combination of ion-exchange high-pressure liquid chromatography (HPLC) and reverse-phase HPLC (RP-HPLC). The molecular mass of toxin was determined by matrix-assisted laser desorption/ionization time-of-flight (MALDI-TOF) mass spectrometry. When the purity of the toxin was determined to be >99%, the peptide of interest (JZTX-III) was collected, lyophilized, and stored at −20 °C until further use.

Functional Expression, Purification, and Identity of Toxins. Recombinant JZTX-III (rJZTX-III) and all JZTX-III mutations have been successfully produced as previously described by Rong et al.[27] The cDNA sequence was retrieved from a venom gland cDNA library of the tarantula *C. jingzhao*.[28] Mutations in the cDNAs encoding JZTX-III mutants were generated by PCR with corresponding synthetic primers bearing the appropriate cDNA clone as template. Sequences of the mutated cDNAs were verified prior to expression by sequencing. Then, the cDNAs were connected into the yeast expression vector pVT102U/α for recombinant plasmid construction and expressed in *Saccharomyces cerevisiae* S-78 (Leu2, Ura3, and Rep4). After fermentation, the supernatant of the culture was adjusted to pH 4.2 with acetic acid. The active toxins in the supernatant were purified using a combination method of ion-exchange and reverse-phase high performance liquid chromatography. Finally, the expressed samples were examined by mass spectrometry to confirm their molecular masses and by CD analysis to estimate their secondary structures. These mutations do not alter the general structure of JZTX-III.

Site-Directed Mutagenesis of Kv2.1. All of the Kv2.1 mutations were constructed using the GeneTailor Site-Directed Mutagenesis System (Invitrogen, Carlsbad, CA, USA) according to the manufacturer's instructions. Site-directed mutations were produced by PCR with corresponding primers. Before mutagenesis reactions, the template plasmids were produced using the plasmid mini kit (OMEGA, USA) and then methylated for 1 h. Each 50 μL reaction mixture contained 0.5 μL of platinum *Taq* high fidelity (5 U/μL), 5 μL of 10 X high fidelity PCR buffer, 1.5 μL of dNTP (10 mM), 1.5 μL of primer mix (10 μM each), and 20 ng of methylated DNA. The PCR conditions were preincubation at 94 °C for 2 min, followed by 20 cycles of 94 °C for 30 s, 55 °C for 30 s, and 68 °C for 10 min, and then a final extension step of 72 °C for 10 min. The PCR products were digested with 1 μL of DpnI for 1 h. All mutations were sequenced to confirm that the appropriate mutations were made.

Electrophysiological Recordings. For the expression in *Xenopus oocytes*, capped RNAs encoding ion channels were synthesized after linearizing the plasmids and performing the transcription by a standard protocol.[29] For in vitro transcription, the plasmids pCI containing the genes for Kv4.1, Kv2.1, and mutant Kv2.1 channels were linearized with NotI; the plasmid PcDNA3.1 containing the gene for Kv4.2 was linearized with *Sma*I; the plasmids pSP64 containing the genes for Kv1.4 and Kv3.1 were linearized with *Eco*RI; and the plasmid pcDNA3.1 containing the gene for Kv4.3 was linearized with *Pst*I. Then, the linearized products were resolved by agarose gel electrophoresis and purified following the instructions in the gel extraction mini kit (OMEGA, USA). Using the linearized plasmids as templates, cRNAs were synthesized in vitro using the large-scale T7 or SP6 mMESSAGE-mMACHINE transcription kit (Ambion, USA) and then purified using the RNA clean up kit (OMEGA, USA).

The harvesting of oocytes from anesthetized female *Xenopus laevis* frogs was as described previously.[25] The oocytes were defolliculated by treatment with 1 mg/mL collagenase for 0.5−1 h in calcium-free ND96 solution (pH 7.43) containing (in mM) NaCl 96, KCl 2, $MgCl_2$ 1, and HEPES 10. The isolated oocytes were incubated in OR_2 solution at 18 °C for microinjection. Then, the oocytes were injected with 18−36 nL of 100−500 ng/μL purified cRNAs using a microprocessor-

controlled nanoliter injector (WPI, USA) and incubated in OR_2 solution (pH 7.43) at 16 °C for 1−4 days. The OR_2 solution contains (in mM) NaCl 82.5, KCl 2.5, $CaCl_2$ 1, Na_2HPO_4 1, $MgCl_2$ 1, and HEPES 5, supplemented with 50 mg/L gentamycin sulfate (only for incubation).

Whole-cell currents from oocytes were recorded using the two-microelectrode voltage clamp (TURBO TEC-03X, NPI Electronic, Germany). Voltage and current electrodes (0.1−1 MΩ) were filled with 3 M KCl. Oocytes were studied in a 100 μL recording chamber that was perfused with OR_2 solution or RbCl solution. RbCl solution contains (in mM) RbCl 50, NaCl 50, $MgCl_2$ 1, $CaCl_2$ 0.3, and HEPES 5 at pH 7.43 with NaOH. Currents were sampled at 20 kHz after low pass filtering at 2 kHz. Linear components of capacity and leak currents were not subtracted. All experiments were performed at room temperature (19 −23 °C).

Data Analysis. Data analysis was performed using the Sigmaplot10.0 (Sigma, St. Louis, MO, USA) software program. All data points are shown as the mean ± standard error (S.E.), and n is the number of independent experiments. Concentration−response curves to determine IC_{50} values were fitted using the Hill logistic equation as follows:

$$y = 1 - (1 - f_{max})/(1 + ([Tx]/IC_{50})^n) \quad (1)$$

where IC_{50} is half-maximal inhibitory concentration, n is an empirical Hill coefficient, and f_{max} is the fraction of current resistant to inhibition at high toxin concentration [Tx]. Voltage−activation relationship (I−V) curves were fitted using the Boltzmann equation as follows:

$$I/I_{max} = 1/[1 + \exp((V - V_{1/2})/k)] \quad (2)$$

in which V is the test potential, $V_{1/2}$ is the potential for half-maximum activation, and k is the slope factor.

Molecular Modeling. The Kv2.1 homology model was constructed using a method similar to that described in the recently published paper by Panpan Hou et al.[30] The Nav1.5 homology model was generated using MODELER[31] with the refined crystal structure of bacterial voltage-gated sodium channel NaChBac (PDB ID: 4DXW)[32] as the template. Then, the course model was optimized in bilayer POPC lipid membrane by the DESMOND molecular dynamics suite.[33] The dockings of the optimized JZTX-III to the Kv2.1 and Nav1.5 homology models were performed using Rosetta.[34] First, a calibration run of 5000 was conducted, which served as a reference set for the whole 20K run. In the following 50K run, the "smart scorefilter 0.04" flag was used to generate 2000 decoys. Then, the structure was extracted for these 2000 decoys, and cluster analysis was done after that. There were 150 clusters from the docking process of JZTX-III/Kv2.1 with the largest cluster containing 92 poses and 108 clusters from JZTX-III/Nav1.5 docking with the largest cluster containing 78 poses. Again molecular dynamics simulations were performed with DESMOND based on a standard Dynamics Cascade pipeline for the simulation of macromolecular systems. The detailed structural conformations of Kv2.1/JZTX-III and Nav1.5/JZTX-III complexes were prepared and rendered by the latest PyMOL Suite (The PyMOL Molecular Graphics System, Version 1.5.0.4 Schrödinger, LLC.).

RESULTS

Functional Characterization of Recombinant JZTX-III. Recombinant JZTX-III (rJZTX-III) was successfully expressed in yeast *S.cerevisiae* S-78 (Supporting Information, Table S1). Compared to native JZTX-III (nJZTX-III), rJZTX-III not only exhibited the same three-dimensional structure but also the same binding affinity for voltage-gated sodium channel Nav1.5.[27] Using the two-microelectrode voltage clamp technique, we first measured the effects of rJZTX-III on Kv2.1 channels. Kv2.1 currents were elicited by a 300-ms depolarization of −10 mV from a holding potential of −80 mV every 5 s. Figure 1A shows the blocking effect of rJZTX-III on

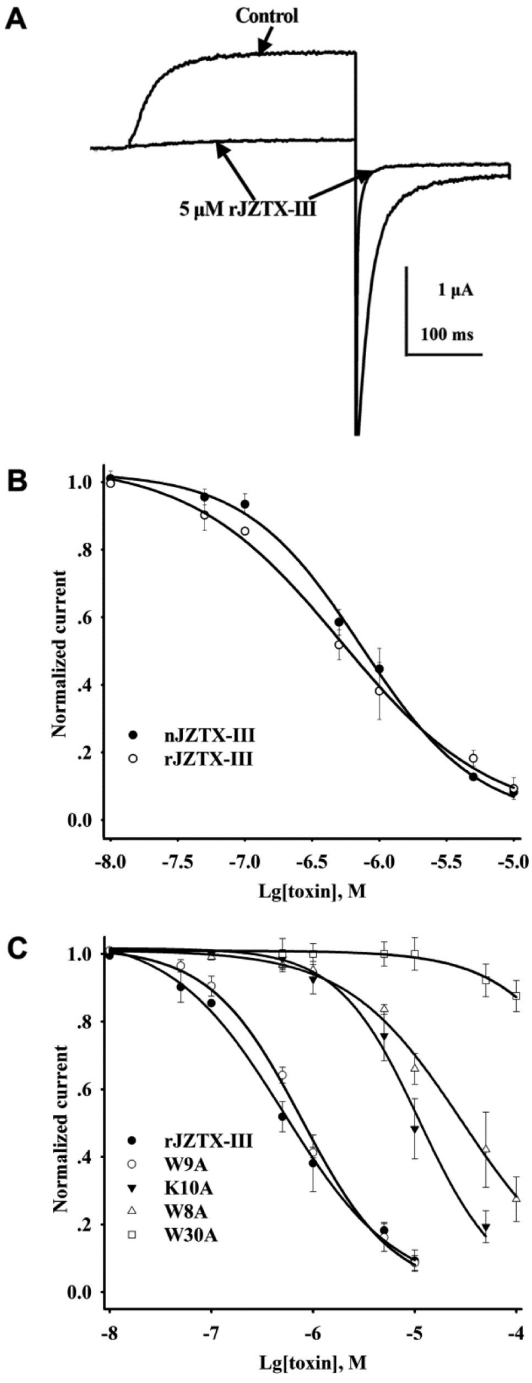

Figure 1. (A) Currents were recorded before and after the application of 5 μM rJZTX-III. (B) Concentration dependence for the inhibition of Kv2.1 currents by both rJZTX-III (○; n = 3) and nJZTX-III (●; n = 3). (C) Dose−response curves of JZTX-III and JZTX-III mutants inhibiting Kv2.1.

dx.doi.org/10.1021/bi4006418 | Biochemistry 2013, 52, 7439−7448

Table 1. Interactions between JZTX-III Mutants and Kv2.1[a]

toxin	IC_{50} (μM)[b]	Mut IC_{50}/WT IC_{50}	inhibition (%)	M
R-JZTX-III (n = 3)	0.54 ± 0.12		88.51 ± 0.02	5×10^{-6}
D1A(n = 4)	0.95 ± 0.13	1.75	70.23 ± 0.02	5×10^{-6}
E3A(n = 4)	4.07 ± 0.07	7.52	61.01 ± 0.03	5×10^{-6}
W8A(n = 4)	27.73 ± 0.09	51.25	72.54 ± 0.07	1×10^{-4}
W9A(n = 4)	0.45 ± 0.18	0.82	83.82 ± 0.04	5×10^{-6}
K10A(n = 4)	9.76 ± 0.05	18.04	51.67 ± 0.09	1×10^{-5}
R13A(n = 3)	94.75 ± 0.01	175.13	53.92 ± 0.12	1×10^{-4}
R13E(n = 4)	22.87 ± 0.38	42.27	37.29 ± 0.07	1×10^{-5}
K15A(n = 3)	>100	>200	0.01 ± 0.01	1×10^{-4}
K20A (n = 3)	6.97 ± 0.04	12.88	77.48 ± 0.02	1×10^{-5}
K26A(n = 3)	6.87 ± 0.01	12.69	69.31 ± 0.05	1×10^{-5}
W28A(n = 3)	>100	>200	2.88 ± 0.03	1×10^{-4}
W30A(n = 4)	>100	>200	12.43 ± 0.05	1×10^{-4}
V33A(n = 3)	>100	>200	16.45 ± 0.10	1×10^{-4}
E34A(n = 3)	>100	>200	13.75 ± 0.002	1×10^{-4}
E34S(n = 3)	>100	>200	1.17 ± 0.01	1×10^{-4}

[a]Activity analysis of JZTX-III mutants on Kv2.1 currents expressed in *Xenopus laevis* oocytes. [b]The IC_{50} values were estimated by fitting the data points to the Hill logistic equation. The mutants with high IC_{50} and Mut IC_{50}/WT IC_{50} values show low affinity for Kv2.1. The data on the right show the probability of current inhibition at corresponding toxin concentration (M).

Kv2.1. At 5 μM concentration, rJZTX-III obviously depressed Kv2.1's current amplitude by 88.51 ± 2%. The IC_{50} value for rJZTX-III was determined to be 0.54 ± 0.12 μM (n = 3), which is close to the value of nJZTX-III (IC_{50} = 0.71 ± 0.01 μM; n = 3) (Table 1 and Figure 1B). Therefore, our data indicated that the recombinant toxin has the same biological function on Kv2.1 as nJZTX-III.

Mutational Analysis of JZTX-III. In our previous work, mutation of all amino acid residues in JZTX-III except Cys, Ala, and Gly to Ala did not exhibit a significant change in the three-dimensional structure.[27] In order to map the active surface of JZTX-III binding to Kv2.1, we successfully expressed 15 JZTX-III mutants in yeast *S. cerevisiae* S-78 (Supporting Information, Table S1) and measured the effects of these mutations on the WT Kv2.1 channel. All mutations were tested at concentrations ranging from 10 nM to 100 μM. The concentration-dependent curves are shown in Figure 1C, and the estimated IC_{50} values are summarized in Table 1. The IC_{50} values of D1A and W9A were close to the value of nJZTX-III, suggesting that Asp1 and Trp9 might not be involved in the JZTX-III interactions with Kv2.1 (n = 4). However, alanine replacement of four charged residues (Glu3, Lys10, Lys20, and Lys26) reduced toxin binding affinity by 8-, 18-, 13-, and 13-fold, respectively (Table 1 and Figure 1C). Compared to these four residues, the residues Trp8 and Arg13 played more important roles in JZTX-III binding to Kv2.1 because the mutations W8A and R13A increased the IC_{50} value by 51- and 175-fold, respectively (Table 1 and Figure 1C). Although R13A mutation did not significantly affect the ability of JZTX-III to bind to Nav1.5, the substitution of Arg13 with Glu could potentiate toxin sensitivity up to 10-fold.[27] Surprisingly, our findings demonstrated that both R13A and R13E reduced toxin binding affinity toward Kv2.1 by >42-fold (Table 1). Each of the five mutations (K15A, W28A, W30A, V33A, and E34A) almost abolished the ability of JZTX-III to block Kv2.1. Even when the concentration of these mutant toxins was increased up to 100 μM, less than 16.5% of Kv2.1 currents were depressed (Table 1 and Figure 1C). Conversion of Lys15, Trp28, Trp30, Val33, and Glu34 to alanine was roughly estimated to reduce toxin binding affinity by <200-fold. Like the mutant E34A, the E34S mutation failed to evidently block Kv2.1.

Alanine-Scanning Mutagenesis of the S1−S2 Linker and the Voltage-Sensor Paddle (S3b-S4). As a gating modifier of Kv2.1 channel, JZTX-III could shift channel activation to more positive voltages and accelerate the transition rate from the open to the closed state.[25] However, in comparison with HaTx1 (K_d ≈ 100 nM)[17] and GxTX-1E (IC_{50} ≈ 4 nM),[35] the toxin exhibited much lower binding affinity for Kv2.1. In order to elucidate the molecular mechanism of JZTX-III binding to the voltage-sensing domain of Kv2.1, we mutated each residue in the S1−S2 linker and the voltage-sensor paddle (S3b-S4) in Kv2.1 using the alanine-scanning technique (Figure 2). As shown in Figure 2B and C, the mutagenesis results for JZTX-III interacting with Kv2.1

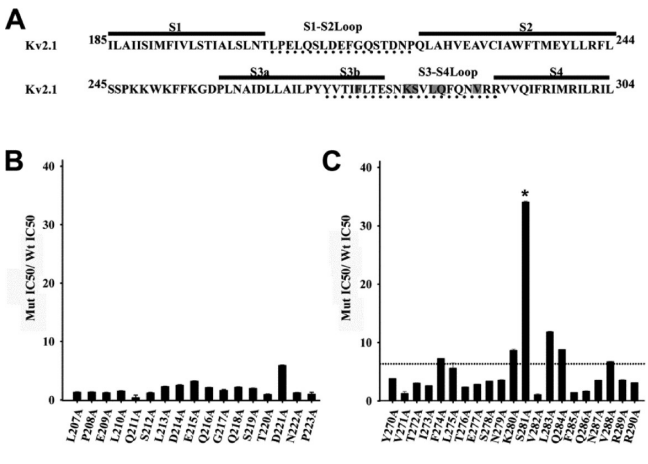

Figure 2. (A) Amino acid residues in the S1−S4 segments of the Kv2.1 channel. Alanine scanning of the S1−S2 linker (B) and the paddle-motif (S3b-S4) (C) in Kv2.1. Changes in apparent toxin affinity (Mut IC_{50}/WT IC_{50}) were plotted for individual mutants. The mutated residues are marked with dotted lines. Six crucial determinants of JZTX-III binding to Kv2.1 are shade in gray. The most crucial residue S281 is marked with *. The dotted line marks a value of 6.

dx.doi.org/10.1021/bi4006418 | *Biochemistry* 2013, 52, 7439−7448

identified six residues in the voltage-sensor paddle that were critical for JZTX-III binding, including F274, K280, S281, L283, Q284, and V288, and alanine mutations of these six residues reduced toxin sensitivity by 7-, 9-, 34-, 12-, 9-, and 7-fold, respectively. However, all other mutants decreased toxin binding affinity by <6-fold. These findings suggested that JZTX-III docks at the voltage-sensor paddle of Kv2.1. The action of JZTX-III on mutant Kv2.1 channels was in a concentration-dependent manner. As can be seen in Figure 3A and B, fitting the data points with a Hill logistic equation determined that the IC_{50} values were 5.16 ± 0.01 (n = 4), 6.16 ± 0.18 (n = 5), 24.19 ± 0.14 (n = 5), 8.40 ± 0.12 (n = 5), 6.25 ± 0.02 (n = 3), and 4.78 ± 0.05 (n = 4) μM for F274A, K280A, S281A, L283A, Q284A, and V288A, respectively. Five micromolar JZTX-III inhibited 94.8 ± 0.5% of the WT Kv2.1 currents (Figure 4A), whereas it only inhibited the mutant S281A currents by 4.4 ± 2.0% (Figure 4B). Effects of 5 μM JZTX-III on the current−voltage (I−V) curves of WT Kv2.1 and mutant S281A were shown in Figure 4C and D, respectively. From the curves, it can be seen that no shift was observed for the mutation S281A (n = 5), although a positive shift of +57 mV was detected on WT Kv2.1 (n = 3).

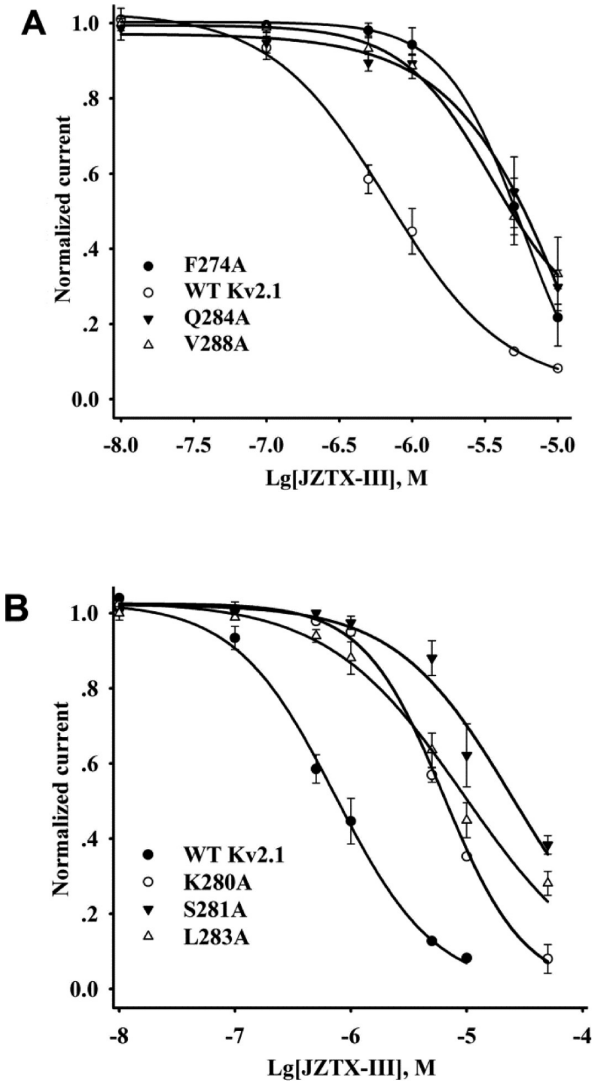

Figure 3. Concentration dependence for the inhibition of three Kv2.1 mutants (F274A, Q284A, and V288A) in A and three Kv2.1 mutants (K280A, S281A, and L283A) in B by JZTX-III.

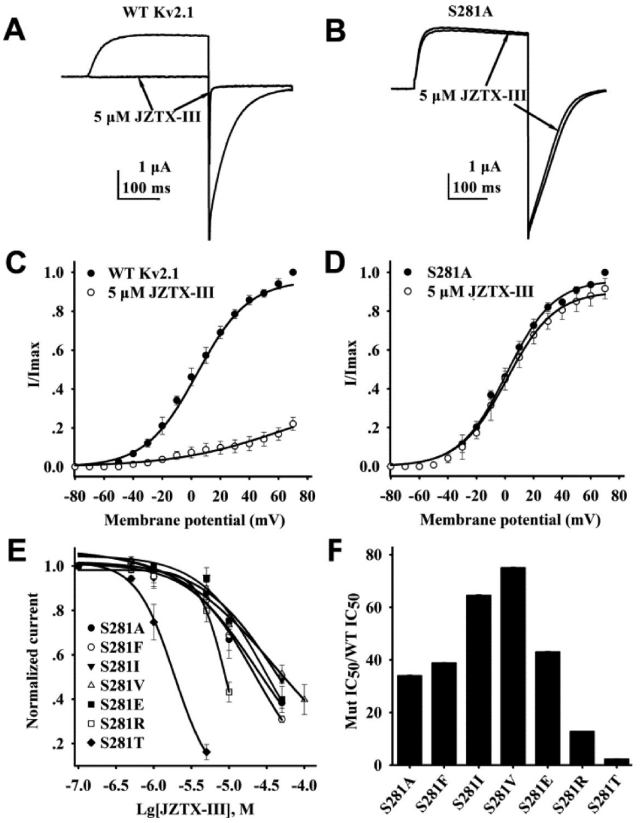

Figure 4. Currents through WT Kv2.1 (A) and mutant S281A (B) were recorded before and after the application of 5 μM JZTX-III. Normalized current−voltage (I−V) relationships for WT Kv2.1(C) and S281A mutation (D) before (●) and after the addition of 5 μM JZTX-III (○). (E) Concentration dependence for the inhibition of seven Kv2.1 mutants by JZTX-III. (F) Normalized IC_{50} values for seven substitutions at position 281.

Effects of Multiple Substitutions at Position 281. To better understand the molecular mechanism of inhibition of Kv2.1 by JZTX-III, we replaced the residue Ser at position 281 by a Phe, Ile, Val, Glu, Arg, and Thr, and the effects of these mutations on JZTX-III binding affinity for Kv2.1 were further investigated. As can be seen in Figure 4E, the IC_{50} values were estimated to be 27.63 ± 0.19 (S281F; n = 3), 45.86 ± 0.20 (S281I; n = 3), 53.28 ± 0.15 (S281V; n = 3), 30.57 ± 0.11 (S281E; n = 4), 9.16 ± 0.01 μM (S281R; n = 4), and 1.59 ± 0.04 μM (S281T; n = 4), respectively, suggesting that compared to WT Kv2.1, toxin binding affinity was reduced by 39-, 65-, 75-, 43-, 13-, and 2-fold, respectively (Figure 4F). Taken together with our electrophysiological analysis on S281A mutation, the order for the IC_{50} values was S ≈ T < R<A < F < E < I < V (Figure 4F). These results indicated that the hydrogen-bonded side chain of S281 may be an important determinant for JZTX-III binding affinity.

Effects of JZTX-III on Other Voltage-Gated Potassium Channels. Previously, we reported that JZTX-III had no effect on potassium channel isoforms Kv1.1, Kv1.2, and Kv1.3.[24] In this study, the effects of JZTX-III on five other potassium channel isoforms (Kv1.4, Kv3.1, Kv4.1, Kv4.2, and Kv4.3) were measured. In the presence of 5 or 10 μM JZTX-III, no significant change was detected, indicating that Kv1.4, Kv3.1,

dx.doi.org/10.1021/bi4006418 | Biochemistry 2013, 52, 7439−7448

Kv4.1, Kv4.2, and Kv4.3 might be resistant to JZTX-III (Figure 5).

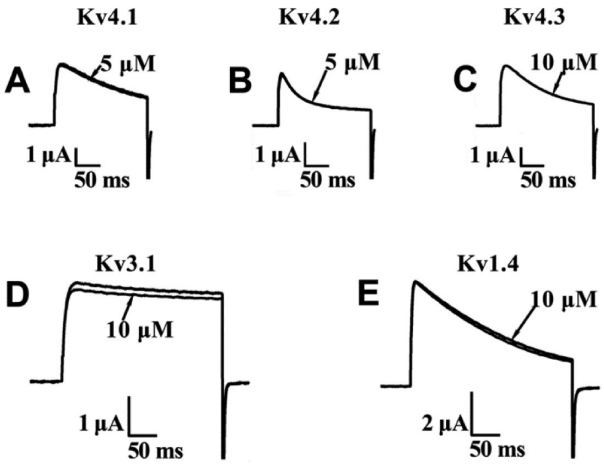

Figure 5. Potassium channel currents were evoked by a 200-ms depolarization from a holding potential of −90 mV to 0 mV for Kv4.1 and Kv4.3, −10 mV for Kv1.4, and +20 mV for Kv4.2. Kv3.1 currents were elicited by a 300-ms depolarization to +10 mV from a holding potential of −80 mV. After exposure to 5 μM JZTX-III, no change of the currents was detected for Kv4.1 (A) and Kv4.2 (B). In the presence of 10 μM JZTX-III, Kv4.3 (C), Kv3.1 (D), and Kv1.4 (E) current traces were not changed.

Dockings of JZTX-III to the Voltage-Sensor Paddles of Kv2.1 and Nav1.5DII. In order to further clarify the underlying interaction mechanisms of JZTX-III with Kv2.1 and Nav1.5 channels, we constructed homology models for Kv2.1 and Nav1.5 as described in the methods and performed docking studies. Obviously, the docking modes were consistent with our present and previous mutagenesis data (Figure 6). As can be seen in Figure 6A, an aromatic ring of residue W9 forms a hydrophobic interaction with residue L804 in Nav1.5. Similarly, residues W8 and W30 in JZTX-III make hydrophobic contacts with V288 and Q284 in Kv2.1, respectively (Figure 6B). In the JZTX-III-Nav1.5 interaction model (Figure 6A), the amino group of R800 is able to interact favorably with the carboxyl group of E3 by forming a salt bridge. This result is quite consistent with our mutational finding[27] that R800 (in Nav1.5) plays the most crucial role in JZTX-III binding. Interestingly, docking of JZTX-III to Kv2.1 also shows that the amino group of K280 forms a salt bridge or a hydrogen bond with the carboxyl group of E34 and that the latter residue might form a hydrogen bond with F274 (Figure 6B). In addition, our docking model of JZTX-III to Kv2.1 further suggests that the most crucial receptor residue S281 can form a good hydrogen bond with the aromatic ring of residue W28 in JZTX-III (Figure 6B), consistent with our experimental findings that multiple S281 mutations significantly altered toxin sensitivity. Positively charged residues in Kv gating modifiers are recently reported to bind to phospholipids of the lipid membrane, therefore increasing toxin binding affinity for ion channels.[36−38] On the basis of our docking model of JZTX-III to Kv2.1 S3−S4 paddle (Figure 6B) and the structural comparison shown in Figure 7, we therefore propose that two basic residues (R13 and K15) in JZTX-III might be primarily important for facilitating entry into the phospholipid bilayer. Hydrophobic interactions, hydrogen bonds, and electrostatic interactions effectively lock the toxin in these positions so that the substituted residues cannot form favorable interactions within the toxin−channel complexes. Therefore, these docking results, together with the data from point mutation experiments, demonstrated that the mode of action of JZTX-III with Kv2.1 is similar to that of the toxin with Nav1.5.

DISCUSSION

The present study aimed to investigate the molecular interactions of JZTX-III with Kv2.1 and clarify the molecular basis for JZTX-III exhibiting cross-activities on Kv2.1 and Nav1.5 channels. Structural comparison in Figure 7 showed that a similar bioactive surface is conserved in other Kv inhibitors. In SGTx1, a hydrophobic patch formed by L5, F6, and W30 has been shown to be important for the toxin partitioning into a lipid membrane and targeting its receptor site on the voltage-sensor paddle.[39−41] Mapping the bioactive surface of JZTX-III targeting Kv2.1 clearly indicated that four hydrophobic residues are crucially involved in JZTX-III binding. Three Trp residues at positions 8, 28, and 30 in JZTX-III correspond to L5, F6, and W30 in SGTx1, respectively (Figure 7). These JZTX-III mutations do not alter the general structure of JZTX-III.[27] Together with our docking models (Figure 6), it seems likely that membrane partitioning of JZTX-III might be involved in the Kv2.1 inhibition, a mechanism of action similar to that of SGTx1 and HaTx1.[41,42]

Voltage-sensor trapping is extensively believed to be the mechanism underlying the modification of animal toxins on voltage-dependent gating of Kv2.1 channels.[10,11] This mecha-

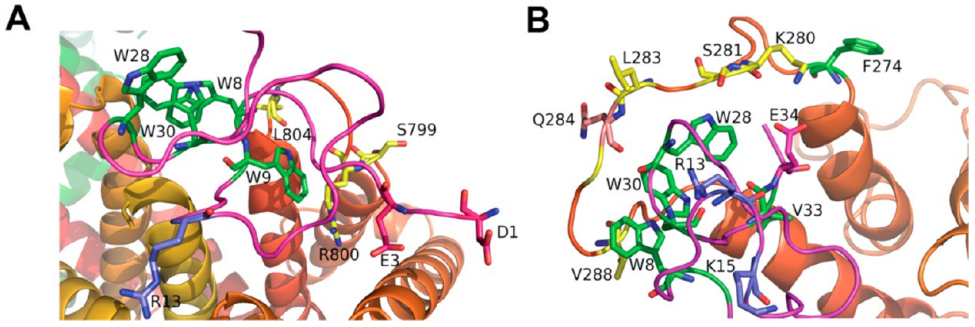

Figure 6. (A) Docking of JZTX-III to the Nav1.5DII voltage sensor with a salt bridge between residues R800 and E3 in JZTX-III and a hydrophobic interaction between the aromatic ring of residues W9 and L804. (B) Docking is shown for JZTX-III to the voltage-sensor paddle of Kv2.1, with a hydrogen bond between residue S281 and the aromatic ring of residue W28 in JZTX-III. The amino group of K280 forms a salt bridge or a hydrogen bond with the carboxyl group of E34. The aromatic rings of W8 and W30 form hydrophobic interactions with residues V288 and Q284, respectively.

dx.doi.org/10.1021/bi4006418 | *Biochemistry* 2013, 52, 7439−7448

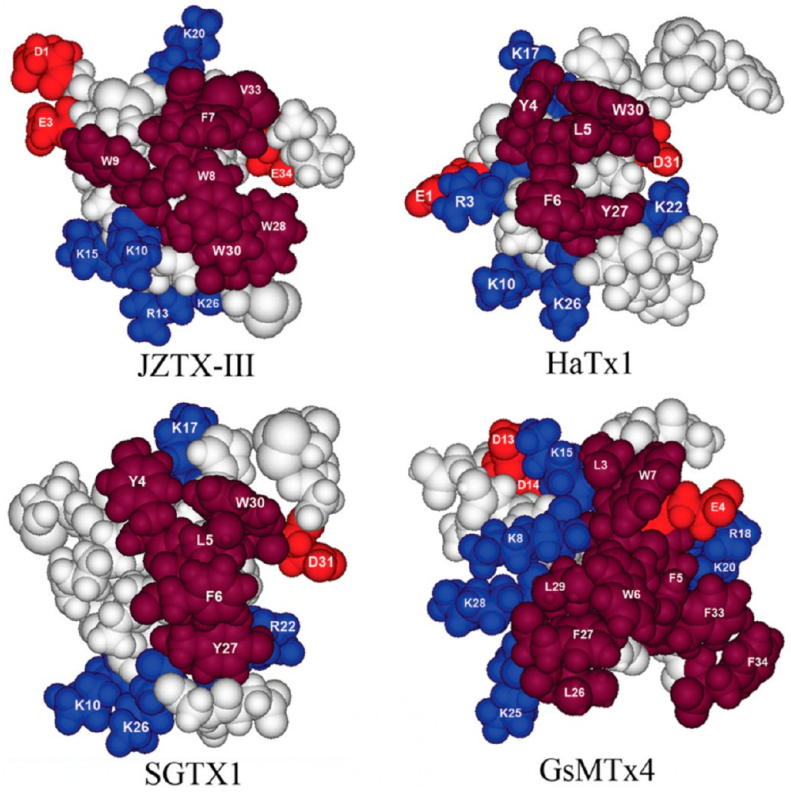

Figure 7. Comparison of three-dimensional structures of SGTx1 (PDB: 1LA4), HaTx1 (PDB: 1D1H), GsMTx4 (PDB: 1TYK), and JZTX-III (PDB: 2I1T). Red, blue, and dark red indicate acidic, basic, and hydrophobic residues, respectively.

nism seems to be commonly used by Kv2.1 gating modifier toxins but does not specify their binding sites. JZTX-III, like HaTx1 and JZTX-I, is a gating modifier toxin of the Kv2.1 channel. Both HaTx1 and JZTX-I bind to Kv2.1 by interacting with crucial residues in S3b, and F274 is the most crucial determinant (Figure 8).[14,15,38] GxTX-1E is another Kv2.1

	S3a	S3b	Linker	S4
HaTx1	PLNAIDLLAILPYYVTI(274)DLTESNKSVLQFQNVRRVVQIFRIMRILRIL			
JZTX-III	PLNAIDLLAILPYYVTIFLTESNK(281)SVLQFQNVRRVVQIFRIMRILRIL			
GxTX-1E	PLNAIDLLAILPYYVTIFLT(277)ESNKSVLQFQNVRRVVQIFRIMRILRIL			
JZTX-I	PLNAIDLLAILPYYVTI(274)DLTESNKSVLQFQNVRRVVQIFRIMRILRIL			

Figure 8. Key molecular determinants for gating modifier toxin binding to Kv2.1. The most crucial residues are shaded in red. All of other key molecular determinants are shaded in gray.

inhibitor that has high homology with JZTX-III (Supporting Information, Figure S1).[18] Interestingly, GxTX-1E is 178-fold more potent than JZTX-III.[35] Previous studies suggested an important role for four residues in the Kv2.1S3b-S4 paddle in the high affinity binding of GxTX-1E (Figure 8).[19] However, our data presented here indicate that JZTX-III primarily docks at the S3−S4 linker with S281 being the major determinant (Figure 8), leading to the suggestion that the binding of JZTX-III differs in that it shares only overlapping, but not identical, determinants on the voltage sensor with these Kv2.1 gating modifiers. E277 and S281 reduced GxTX-1E affinity by almost 150-fold and 30-fold, respectively.[19] Remarkably, although S281 also substantially modulated the interaction of GxTX-1E with Kv2.1, the most key residue E277 was not involved in JZTX-III binding (Figure 8). Furthermore, our mutational data and docking model (Figure 6B), combined with the fact that residue S281 is not significantly involved in the channel−lipid membrane interaction[19] indicated that the JZTX-III−Kv2.1 interaction might depend mainly on the hydrogen bonding ability of S281 by forming a hydrogen bond within the toxin−channel complexes.

In our previous study, we have shown that the functional surface of JZTX-III binding to Nav1.5 is composed of four hydrophobic residues (W8, W9, W28, and W30) and two acidic residues (E3 and D1).[27] When compared with the bioactive surface of JZTX-III targeting Nav1.5 (Figure 9B),[27] the hydrophobic patch formed by residues W8, W28, and W30 is also found in the functionally important surface of JZTX-III interacting with Kv2.1 (Figure 9C). However, interestingly, residues D1, E3, and W9 at the N-terminal of JZTX-III are only important for targeting Nav1.5, whereas R13 and K15 in the middle of the toxin and V33 and E34 at the C-terminal are only crucially involved in the JZTX-III−Kv2.1 interaction (Figure 9A). In Figure 9, the bioactive surface formed by D1, E3 and W9 is totally separated from those formed by R13 and K15 and by V33 and E34. Although JZTX-III exhibited cross-activities on Kv2.1 and Nav1.5, these results indicated that the toxin adopts only partially overlapping bioactive surfaces to target these two different types of ion channels.

JZTX-III might inhibit the activation of Kv2.1 and Nav1.5 channels through similar mechanisms. Similar to Nav1.5 DII, JZTX-III trapped the Kv2.1 voltage sensor at the closed configuration by docking at the voltage-sensor paddle. JZTX-III could accelerate the decay of Kv2.1 tail currents,[25] which reflects the transition from the open to the closed state. In the DIIS3-S4 region of Nav1.5, R800 was a major determinant and formed an electrostatic interaction with an acidic residue in

dx.doi.org/10.1021/bi4006418 | *Biochemistry* 2013, 52, 7439−7448

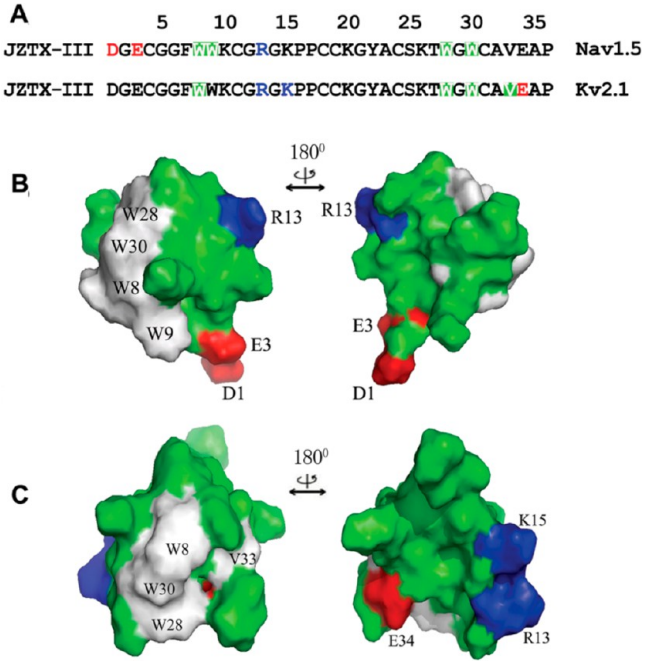

Figure 9. (A) Amino acid sequence of JZTX-III. The important residues for JZTX-III binding to Kv2.1 and Nav1.5 are highlighted and color coded as follows: white (shaded in green), hydrophobic; dark blue, basic; and red, acidic. Numbers above the amino acid sequences show the positions of residues in JZTX-III. (B) Bioactive surface profile of JZTX-III binding to Nav1.5.[27] (C) Bioactive surface profile of JZTX-III binding to Kv2.1. The left and right structures were rotated 180° relative to one another about a vertical axis.

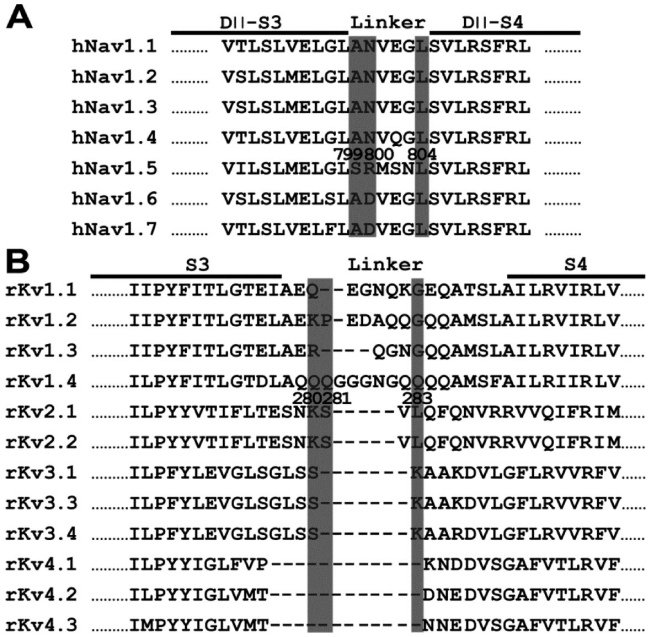

Figure 10. Three important residues (S799, R800, and L804) for JZTX-III binding to Nav1.5DII (A) and three crucial determinants (K280, S281, and L283) for the JZTX-III trapping Kv2.1 voltage sensor (B) are located at the S3−S4 linker. The positions of these crucial determinants are shaded in gray.

JZTX-III.[27] In the S3b-S4 paddle of Kv2.1, the side chain of S281 is critical for JZTX-III binding by forming a hydrogen bond within the JZTX-III−Kv2.1 interaction. Sequence alignment in Figure 10 shows that S281 in Kv2.1 corresponds to R800 in the Nav1.5 DII S3−S4 linker. Although the substitution of S281 with Arg reduced toxin binding affinity by 13-fold, S281R failed to completely abolish the sensitivity of Kv2.1 to JZTX-III. K280 and L283 in Kv2.1 correspond to S799 and L804 in Nav1.5 DII, respectively. The residues at these two positions were also critical for the inhibition of Kv2.1 and Nav1.5 by JZTX-III. Since gating modifiers can interact with a conserved structural motif in Nav and Kv channels,[22,43] we propose that the JZTX-III-binding motif might be conserved in the voltage-sensor paddles of both Kv2.1 and Nav1.5DII. Furthermore, taken together, our results also have defined an essential core toxin-binding motif as S/K-R/S-$X_{(1-3)}$-L, in which X denotes any amino acid residue. Given the fact that the core motif does not emerge in the ion channel subtypes (Nav1.1−1.4, Nav1.6−Nav1.7, Kv1.1−1.4, Kv3.1, and Kv4.1−4.3) (Figure 10), it is not surprising that these ion channel subtypes are resistant to JZTX-III. The voltage-sensor paddle of Kv2.1 is totally identical to that of Kv2.2; we therefore predict that Kv2.2 will also show sensitivity.

In this study, we first investigated the molecular mechanism of animal toxins exhibiting cross-activities on different types of ion channels. JZTX-III selectively inhibited Nav1.5 and Kv2.1 perhaps by recognizing a conserved binding motif on the voltage-sensor paddle. However, unexpectedly, JZTX-III utilized partially overlapping bioactive surfaces to interact with Nav1.5 and Kv2.1, which might result from the divergent amino acid composition of the binding motifs in different ion channels. Therefore, our increased understanding of the interaction mechanisms of JZTX-III with Kv2.1 and Nav1.5 might be valuable to better specify and derive useful peptide pharmacological properties in the future.

■ ASSOCIATED CONTENT

Ⓢ Supporting Information

Values of molecular masses for expressed JZTX-III and JZTX-III mutants and sequence alignment of JZTX-III with HaTx1, GxTX-1E, and JZTX-I. This material is available free of charge via the Internet at http://pubs.acs.org.

■ AUTHOR INFORMATION

Corresponding Author

*Tel: 86-731-88861304. Fax: 86-731-88861304. E-mail: liangsp@hunnu.edu.cn.

Funding

This work was supported by grants from National 973 Project of China (No2010CB529801), Science Research Fund of Hunan Provincial Education Department (10B049), Key Project of Chinese Ministry of Education (No. 208096), Huo Ying Dong Education Foundation (No. 111023), Scientific Research Fund of Hunan Provincial Education Department (10C0961), National Natural Science Foundation of China (31000477), National Natural Science Foundation of China (30900242), and National Natural Science Foundation of China (No. 31100764).

Notes

The authors declare no competing financial interest.

■ ACKNOWLEDGMENTS

We are grateful to Professor Jeanne M. Nerbonne for providing the Kv4.2 and Kv4.3 clones. We thank Professor Sylvie Diochot for providing the Kv2.1 and Kv4.1 clones. Professor Stanley

Nattel kindly provided the Kv1.4 and Kv3.1 clones. We thank Sheng Wang for molecular modeling.

■ ABBREVIATIONS

JZTX-III, Jingzhaotoxin-III; HPLC, high pressure liquid chromatography; nJZTX-III, native JZTX-III; rJZTX-III, recombinant JZTX-III; WT, wide type; *S. cerevisiae*, *Saccharomyces cerevisiae*; TTX-S, tetrodotoxin-sensitive; VGPCs, voltage-gated potassium channels; VSDs, voltage-sensing domains; HaTx1, Hanatoxin1; GxTX-1E, Guangxitoxin-1E

■ REFERENCES

(1) Yellen, G. (2002) The voltage-gated potassium channels and their relatives. *Nature 419*, 35−42.
(2) Swartz, K. J. (2008) Sensing voltage across lipid membranes. *Nature 456*, 891−897.
(3) Doyle, D. A., Cabral, J. M., Pfuetzner, R. A., Kuo, A., Gulbis, J. M., Cohen, S. L., Chait, B. T., and MacKinnon, R. (1998) The structure of the potassium channel: molecular basis of K^+ conduction and selectivity. *Science 280*, 69−77.
(4) Jiang, Y., Lee, A., Chen, J., Ruta, V., Cadene, M., Chait, B. T., and MacKinnon, R. (2003) X-ray structure of a voltage-dependent K^+ channel. *Nature 423*, 33−41.
(5) Long, S. B., Tao, X., Campbell, E. B., and MacKinnon, R. (2007) Atomic structure of a voltage-dependent K^+ channel in a lipid membrane-like environment. *Nature 450*, 376−382.
(6) Long, S. B., Campbell, E. B., and MacKinnon, R. (2005) Crystal structure of a mammalian voltage-dependent shaker family K^+ channel. *Science 309*, 897−903.
(7) Long, S. B., Campbell, E. B., and MacKinnon, R. (2005) Voltage sensor of Kv1.2: structural basis of electromechanical coupling. *Science 309*, 903−908.
(8) Wickenden, A. D. (2002) K^+ channels as therapeutic drug targets. *Pharmacol. Ther. 94*, 157−182.
(9) Shieh, C.-C., Coghlan, M., Sullivan, J. P., and Gopalakrishnan, M. (2000) Potassium channels: molecular defects, diseases, and therapeutic opportunities. *Pharmacol. Rev. 52*, 557−594.
(10) Catterall, W. A., Cestèle, S., Yarov-Yarovoy, V., Yu, F. H., Konoki, K., and Scheuer, T. (2007) Voltage-gated ion channels and gating modifier toxins. *Toxicon 49*, 124−141.
(11) Swartz, K. J. (2007) Tarantula toxins interacting with voltage sensors in potassium channels. *Toxicon 49*, 213−230.
(12) Rodríguez de la Vega, R. C., Merino, E., Becerril, B., and Possani, L. D. (2003) Novel interactions between K^+ channels and scorpion toxins. *Trends. Pharmacol. Sci. 24*, 222−227.
(13) Zhu, S., Peigneur, S., Gao, B., Luo, L., Jin, D., Zhao, Y., and Tytgat, J. (2011) Molecular diversity and functional evolution of scorpion potassium channel toxins. *Mol. Cell. Proteomics 10*, M110−002832.
(14) Swartz, K. J., and MacKinnon, R. (1997) Mapping the receptor site for hanatoxin, a gating modifier of voltage-dependent K^+ channels. *Neuron 18*, 675−682.
(15) Li-Smerin, Y., and Swartz, K. J. (2000) Localization and molecular determinants of the hanatoxin receptors on the voltage-sensing domains of a K^+ channel. *J. Gen. Physiol. 115*, 673−684.
(16) Li-Smerin, Y., and Swartz, K. J. (2001) Helical structure of the COOH terminus of S3 and its contribution to the gating modifier toxin receptor in voltage-gated ion channels. *J. Gen. Physiol. 117*, 205−218.
(17) Lee, H. C., Wang, J. M., and Swartz, K. J. (2003) Interaction between extracellular hanatoxin and the resting conformation of the voltage-sensor paddle in Kv channels. *Neuron 40*, 527−536.
(18) Lee, S., Milescu, M., Jung, H. H., Lee, J. Y., Bae, C. H., Lee, C. W., Kim, H. H., Swartz, K. J., and Kim, J. I. (2010) Solution structure of GxTX-1E, a high-affinity tarantula toxin interacting with voltage sensors in Kv2.1 potassium channels. *Biochemistry 49*, 5134−5142.
(19) Milescu, M., Bosmans, F., Lee, S., Alabi, A. A., Kim, J. I., and Swartz, K. J. (2009) Interactions between lipids and voltage sensor paddles detected with tarantula toxins. *Nat. Struct. Mol. Biol. 16*, 1080−1085.
(20) Winterfield, J. R., and Swartz, K. J. (2000) A hot spot for the interaction of gating modifier toxins with voltage-dependent ion channels. *J. Gen. Physiol. 116*, 637−644.
(21) Li-Smerin, Y., and Swartz, K. J. (1998) Gating modifier toxins reveal a conserved structural motif in voltage-gated Ca^{2+} and K^+ channels. *Proc. Natl. Acad. Sci. U.S.A. 95*, 8585−8589.
(22) Bosmans, F., Martin-Eauclaire, M.-F., and Swartz, K. J. (2008) Deconstructing voltage sensor function and pharmacology in sodium channels. *Nature 456*, 202−208.
(23) Alabi, A. A., Bahamonde, M. I., Jung, H. J., Kim, J. I., and Swartz, K. J. (2007) Portability of paddle motif function and pharmacology in voltage sensors. *Nature 450*, 370−375.
(24) Xiao, Y., Tang, J., Yang, Y., Wang, M., Hu, W., Xie, J., Zeng, X., and Liang, S. (2004) Jingzhaotoxin-III, a novel spider toxin inhibiting activation of voltage-gated sodium channel in rat cardiac myocytes. *J. Biol. Chem. 279*, 26220−26226.
(25) Yuan, C., Yang, S., Liao, Z., and Liang, S. (2007) Effects and mechanism of Chinese tarantula toxins on the Kv2.1 potassium channels. *Biochem. Biophys. Res. Commun. 352*, 799−804.
(26) Liao, Z., Yuan, C., Peng, K., Xiao, Y., and Liang, S. (2007) Solution structure of Jingzhaotoxin-III, a peptide toxin inhibiting both Nav1.5 and Kv2.1 channels. *Toxicon 50*, 135−143.
(27) Rong, M., Chen, J., Tao, H., Wu, Y., Jiang, P., Lu, M., Su, H., Chi, Y., Cai, T., Zhao, L., Zeng, X., Xiao, Y., and Liang, S. (2011) Molecular basis of the tarantula toxin jingzhaotoxin-III (β-TRTX-Cj1α) interacting with voltage sensors in sodium channel subtype Nav1.5. *FASEB J. 25*, 3177−3185.
(28) Chen, J., Deng, M., He, Q., Meng, E., Jiang, L., Liao, Z., Rong, M., and Liang, S. (2008) Molecular diversity and evolution of cystine knot toxins of the tarantula *Chilobrachys jingzhao*. *Cell. Mol. Life. Sci. 65*, 2431−2444.
(29) Krieg, P. A., and Melton, D. A. (1987) In vitro RNA synthesis with SP6 RNA polymerase. *Methods. Enzymol. 155*, 397−415.
(30) Hou, P., Zeng, W., Gan, G., Lv, C., Guo, X., Zhang, Z., Liu, H., Wu, Y., Yao, J., Wei, A. D., Wang, S., and Ding, J. (2013) Inter-α/β subunits coupling mediating pre-inactivation and augmented activation of BKCa(β2). *Sci. Rep. 3*, 01666.
(31) Šali, A., and Blundell, T. L. (1993) Comparative protein modelling by satisfaction of spatial restraints. *J. Mol. Biol. 234*, 779−815.
(32) Zhang, X., Ren, W., DeCaen, P., Yan, C., Tao, X., Tang, L., Wang, J., Hasegawa, K., Kumasaka, T., He, J., Wang, J., Clapham, D. E., and Yan, N. (2012) Crystal structure of an orthologue of the NaChBac voltage-gated sodium channel. *Nature 486*, 130−134.
(33) Bowers, K. J., Chow, E., Huageng, X., Dror, R. O., Eastwood, M. P., Gregersen, B. A., Klepeis, J. L., Kolossvary, I., Moraes, M. A., Sacerdoti, F. D., Salmon, J. K., Yibing, S., and Shaw, D. E. (2006) Scalable Algorithms for Molecular Dynamics Simulations on Commodity Clusters, in *SC 2006 Conference, Proceedings of the ACM/IEEE*, pp 43−43, ACM, New York.
(34) Das, R., André, I., Shen, Y., Wu, Y., Lemak, A., Bansal, S., Arrowsmith, C. H., Szyperski, T., and Baker, D. (2009) Simultaneous prediction of protein folding and docking at high resolution. *Proc. Natl. Acad. Sci. U.S.A. 106*, 18978−18983.
(35) Herrington, J., Zhou, Y.-P., Bugianesi, R. M., Dulski, P. M., Feng, Y., Warren, V. A., Smith, M. M., Kohler, M. G., Garsky, V. M., Sanchez, M., Wagner, M., Raphaelli, K., Banerjee, P., Ahaghotu, C., Wunderler, D., Priest, B. T., Mehl, J. T., Garcia, M. L., McManus, O. B., Kaczorowski, G. J., and Slaughter, R. S. (2006) Blockers of the delayed-rectifier potassium current in pancreatic β-cells enhance glucose-dependent insulin secretion. *Diabetes 55*, 1034−1042.
(36) Nishizawa, M., and Nishizawa, K. (2006) Interaction between K^+ channel gate modifier hanatoxin and lipid bilayer membranes analyzed by molecular dynamics simulation. *Eur. Biophys. J. 35*, 373−381.
(37) Nishizawa, M., and Nishizawa, K. (2007) Molecular dynamics simulations of a stretch-activated channel inhibitor GsMTx4 with lipid

membranes: two binding modes and effects of lipid structure. *Biophys. J. 92*, 4233−4243.
(38) Tao, H., Wu, Y., Deng, M., He, J., Wang, M., Xiao, Y., and Liang, S. (2013) Molecular determinants for the tarantula toxin jingzhaotoxin-I interacting with potassium channel Kv2.1. *Toxicon 63*, 129−136.
(39) Wang, J. M., Roh, S. H., Kim, S., Lee, C. W., Kim, J. I., and Swartz, K. J. (2004) Molecular surface of tarantula toxins interacting with voltage sensors in Kv channels. *J. Gen. Physiol. 123*, 455−467.
(40) Jung, H. H., Jung, H. J., Milescu, M., Lee, C. W., Lee, S., Lee, J. Y., Eu, Y.-J., Kim, H. H., Swartz, K. J., and Kim, J. I. (2010) Structure and orientation of a voltage-sensor toxin in lipid membranes. *Biophys. J. 99*, 638−646.
(41) Milescu, M., Vobecky, J., Roh, S. H., Kim, S. H., Jung, H. J., Kim, J. I., and Swartz, K. J. (2007) Tarantula toxins interact with voltage sensors within lipid membranes. *J. Gen. Physiol. 130*, 497−511.
(42) Revell Phillips, L., Milescu, M., Li-Smerin, Y., Mindell, J. A., Kim, J. I., and Swartz, K. J. (2005) Voltage-sensor activation with a tarantula toxin as cargo. *Nature 436*, 857−860.
(43) Kopljar, I., Labro, A. J., Cuypers, E., Johnson, H. W. B., Rainier, J. D., Tytgat, J., and Snyders, D. J. (2009) A polyether biotoxin binding site on the lipid-exposed face of the pore domain of Kv channels revealed by the marine toxin gambierol. *Proc. Natl. Acad. Sci. U.S.A. 106*, 9896−9901.